Available online at www.sciencedirect.com
ScienceDirect
International Journal of Heat and Mass Transfer 50 (2007) 1212–1219
International Journal of HEAT and MASS TRANSFER
www.elsevier.com/locate/ijhmt

Technical Note

Meshless element free Galerkin method for unsteady nonlinear heat transfer problems

Akhilendra Singh [a,*], Indra Vir Singh [b], Ravi Prakash [a]

[a] Department of Mechanical Engineering, Birla Institute of Technology and Science, Pilani 333031, Rajasthan, India
[b] Department of Mechanical Systems Engineering, Shinshu University, 4-17-1 Wakasato, Nagano City 380-8553, Japan

Received 15 July 2005; received in revised form 16 August 2006
Available online 21 November 2006

Abstract

In this paper, meshless element free Galerkin (EFG) method has been extended to obtain the numerical solution of nonlinear, unsteady heat transfer problems with temperature dependent material properties. The thermal conductivity, specific heat and density of the material are assumed to vary linearly with the temperature. Quasi-linearization scheme has been used to obtain the nonlinear solution whereas backward difference method is used for the time integration. The essential boundary conditions have been enforced by Lagrange multiplier technique. The meshless formulation has been presented for a nonlinear 3-D heat transfer problem. In 1-D, the results obtained by EFG method are compared with those obtained by finite element and analytical methods whereas in 2-D and 3-D, the results are compared with those obtained by finite element method.

Keywords: Meshless EFG method; Backward difference method; Temperature dependent material properties; Finite element method; Nonlinear heat transfer

1. Introduction

Analysis of nonlinear transient heat transfer problems is very important in practice. It is difficult to find analytical solution for such problems, so the only choice left is approximate numerical solution. A variety of numerical techniques are available to solve these problems.

An FEM based numerical iterative method has been used by Donea and Giuliani [1] to solve steady-state nonlinear heat transfer problems in two-dimensional structures with temperature dependent thermal conductivities and radiative heat transfer. Bathe and Khoshgoftaar [2] have obtained an FEM based numerical solution for the nonlinear steady-state and transient heat transfer problems in which they considered the convection and radiation boundary conditions. Ling and Surana [3] used the *p*-version least square finite element method for obtaining the numerical solution of axisymmetric heat conduction problems with temperature-dependent thermal conductivities. Yang [4] developed an FEM based time integration algorithm for the solution of nonlinear heat transfer problems. Homotophy analysis method has been improved and applied by Liao [5] to solve strongly nonlinear heat transfer problems. Transient heat conduction and radiation heat transfer problems with variable thermal conductivity have been solved by Talukdar and Mishra [6] using discrete transfer and implicit schemes. Bondarev [7] has used variational calculation method to solve unsteady state strong nonlinear problems in heat conduction. General boundary element method has been used by Liao [8] to solve nonlinear heat transfer problems governed by hyperbolic heat conduction equation. Skerget and Alujevic [9] uses boundary element method to solve nonlinear transient heat transfer in reactor solids with convection and radiation on surfaces. The further use of general boundary element

* Corresponding author. Tel.: +91 1596 245073x225; fax: +91 1596 244183.
E-mail addresses: akhilendra.singh@gmail.com (A. Singh), iv_singh@yahoo.com (I.V. Singh).

0017-9310/$ - see front matter © 2006 Elsevier Ltd. All rights reserved.
doi:10.1016/j.ijheatmasstransfer.2006.08.039

Nomenclature

$C(T)$	specific heat, J/kg °C
C_0	reference specific heat, J/kg °C
$d_{\max}$	scaling parameter
$k(T)$	thermal conductivity, W/m °C
k_0	reference thermal conductivity, W/m °C
m	number of terms in the basis function
n	number of nodes in the domain of influence
$\bar{n}$	number of iterations
$p_j(\mathbf{x})$	monomial basis function
q	heat flux, W/m^2
$\dot{Q}$	rate of internal heat generation per unit volume, W/m^3
$\bar{r}$	normalized radius
$\dot{T}$	$\frac{\partial T}{\partial t}$
t	time, s
Δt	time step-size, s
$T^h(\mathbf{x})$	moving least square approximant
V	three-dimensional domain
$w(\mathbf{x}-\mathbf{x}_I)$	weight function used in MLS approximation
$\bar{w}$	weighting function used in weak formulation

Greek symbols

β_1	coefficient of thermal conductivity variation, °C
β_2	coefficient of specific heat variation, °C
β_3	coefficient of density variation, °C
Ω	two-dimensional domain
$\Phi_I(\mathbf{x})$	shape function
λ	Lagrangian multiplier
$\rho(T)$	density, kg/m^3
ρ_0	reference density, kg/m^3

method has been done by Liao and Chwang [10] to solve strongly nonlinear heat transfer problems. A low order spectral method has been used by Siddique and Khayat [11] to solve nonlinear heat conduction problems with periodic boundary conditions and periodic geometry. The precise time integration (PTI) method has been introduced by Chen et al. [12] and applied to linear and nonlinear transient heat conduction problems with temperature dependent thermal conductivity and predictor-corrector algorithm is employed to solve the nonlinear equations, etc. Out of all the numerical methods developed so far, finite element method has been found the most general method not only to solve the problems of nonlinear heat transfer but also to solve the various problems in different areas of engineering and sciences. In spite of its numerous advantages, it is not well-suited for certain class of problems such as crack propagation, dynamic impact problems, moving phase boundaries, phase transformation, large deformations, modeling of multi-scale phenomena, and nonlinear thermal analysis. To overcome these problems, a number of meshless methods have been developed in last two decades. These methods have the following advantages over FEM [13]:

- Only nodal data is required for the interpolation of field variables.
- No mesh or elements are involved in the discretization process.
- Node insertion or elimination is quite easier than FEM.
- No need of tedious and time consuming re-meshing process.
- No volumetric locking problem due to unavailability of elements.
- Selection of basis function is more flexible than FEM.
- Complex geometries and moving domain problems can be easily handled.
- Smooth shape functions are used based on local approximation.
- Good accuracy and high convergence rate can be achieved.
- Post-processing for the results is quite smooth.

Although most of the meshless methods have high computational cost as compared to FEM, but above advantages of meshless methods over FEM have motivated us to extend the application of meshless method in unsteady state nonlinear heat transfer. In the present work, element free Galerkin (EFG) method has been used due to its good accuracy, ease in formulation, and wide range of applications [14,15], and to start with, simple geometries have been chosen in 1-D, 2-D and 3-D. For nonlinear simulation, it is assumed that material properties i.e. thermal conductivity, specific heat and density are varying linearly with temperature. Lagrange multiplier method has been used to enforce the essential boundary conditions. The meshless formulation has been given for a 3-D model problem. The discrete equations are obtained using variational principle approach. In 1-D problem, the results obtained by EFG method are compared with those obtained by finite element [ANSYS 8.0] and analytical methods [16], whereas in case of 2-D and 3-D problems, the results are compared with those obtained by finite element method [ANSYS 8.0].

2. Review of element free Galerkin method

The EFG method utilizes the moving least square (MLS) approximants, which are constructed in terms of nodes only. The MLS approximation consists of three components: a basis function, a weight function associated with each node, and a set of coefficients that depends on node position. Using MLS approximation, an unknown

temperature function $T(\mathbf{x})$ is approximated by $T^h(\mathbf{x})$ [14,15]:

$$T^h(\mathbf{x}) = \sum_{j=1}^{m} p_j(\mathbf{x}) a_j(\mathbf{x}) \equiv \mathbf{p}^{\mathrm{T}}(\mathbf{x})\mathbf{a}(\mathbf{x}) \tag{1}$$

where $\mathbf{p}^{\mathrm{T}}(\mathbf{x}) = [1, x, y, z]$, $\mathbf{a}^{\mathrm{T}}(\mathbf{x}) = [a_1(\mathbf{x}), a_2(\mathbf{x}), a_3(\mathbf{x}), a_4(\mathbf{x})]$, m is the number of terms in the basis function. At any given point $\mathbf{x}$, the unknown coefficients $\mathbf{a}(\mathbf{x})$ are determined by minimizing the weighted discrete L_2-norm J:

$$J = \sum_{I=1}^{n} w(\mathbf{x} - \mathbf{x}_I)[\mathbf{p}^{\mathrm{T}}(\mathbf{x})\mathbf{a}(\mathbf{x}) - T_I]^2 \tag{2}$$

where T_I is the nodal parameter at $\mathbf{x} = \mathbf{x}_I$, it is not the nodal value of $T^h(\mathbf{x} = \mathbf{x}_I)$ since $T^h(\mathbf{x})$ is an approximant not an interpolant; $w(\mathbf{x} - \mathbf{x}_I)$ is a non-zero weight function of node I at $\mathbf{x}$ and n is the number of nodes in the domain of influence of $\mathbf{x}$ for which $w(\mathbf{x} - \mathbf{x}_I) \neq 0$. The stationary value of J in Eq. (2) with respect to $\mathbf{a}(\mathbf{x})$ leads to the following set of linear equations:

$$\mathbf{A}(\mathbf{x})\mathbf{a}(\mathbf{x}) = \mathbf{B}(\mathbf{x})\mathbf{T} \tag{3}$$

where $\mathbf{A}$ and $\mathbf{B}$ are given as

$$\mathbf{A} = \sum_{I=1}^{n} w(\mathbf{x} - \mathbf{x}_I)\mathbf{p}(\mathbf{x}_I)\mathbf{p}^{\mathrm{T}}(\mathbf{x}_I) \tag{4}$$

$$\mathbf{B}(\mathbf{x}) = \{w(\mathbf{x} - \mathbf{x}_1)\mathbf{p}(\mathbf{x}_1), w(\mathbf{x} - \mathbf{x}_2)\mathbf{p}(\mathbf{x}_2), \ldots, w(\mathbf{x} - \mathbf{x}_n)\mathbf{p}(\mathbf{x}_n)\} \tag{5}$$

Substituting $\mathbf{a}(\mathbf{x})$ in Eq. (1), the MLS approximant is obtained as

$$T^h(\mathbf{x}) = \sum_{I=1}^{n} \Phi_I(\mathbf{x}) T_I = \Phi^{\mathrm{T}}(\mathbf{x})\mathbf{T} \tag{6}$$

where

$$\Phi^{\mathrm{T}}(\mathbf{x}) = \{\Phi_1(\mathbf{x}), \Phi_2(\mathbf{x}), \Phi_3(\mathbf{x}), \ldots, \Phi_n(\mathbf{x})\} \tag{7}$$

$$\mathbf{T}^{\mathrm{T}} = [T_1, T_2, T_3, \ldots, T_n] \tag{8}$$

The mesh free shape function $\Phi_I(\mathbf{x})$ is defined as

$$\Phi_I(\mathbf{x}) = \sum_{j=1}^{m} p_j(\mathbf{x})(\mathbf{A}^{-1}(\mathbf{x})\mathbf{B}(\mathbf{x}))_{jI} = \mathbf{p}^{\mathrm{T}}\mathbf{A}^{-1}\mathbf{B}_I \tag{9}$$

2.1. The weight function

The weight function is non-zero over a small neighborhood of a node $\mathbf{x}_I$ called the support or domain of influence of node I. The exponential weight function [15] used in present analysis can be written as a function of normalized radius $\bar{r}$ as

$$w(\bar{r}) = \begin{Bmatrix} 100^{-\bar{r}} & 0 \leqslant \bar{r} \leqslant 1 \\ 0 & \bar{r} > 1 \end{Bmatrix} \tag{10}$$

where $\bar{r}_I = \|\mathbf{x} - \mathbf{x}_I\|/d_{mI}$ and $\|\mathbf{x} - \mathbf{x}_I\|$, is the distance from a sampling point $\mathbf{x}$ to a node $\mathbf{x}_I$, and d_{mI} is the domain of influence of node I. $(\bar{r}_x)_I = \|x - x_I\|/d_{mxI}$, $(\bar{r}_y)_I = \|y - y_I\|/d_{myI}$, $(\bar{r}_z)_I = \|z - z_I\|/d_{mzI}$, $d_{mxI} = d_{\max} c_{xI}$, $d_{myI} = d_{\max} c_{yI}$, $d_{mzI} = d_{\max} c_{zI}$, $d_{\max}$ = scaling parameter. c_{xI}, c_{yI} and c_{zI} at node I, are the distances to the nearest neighbors. The weight function at any given point is obtained as

$$w(\mathbf{x} - \mathbf{x}_I) = w(\bar{r}_x)w(\bar{r}_y)w(\bar{r}_z) = w_x w_y w_z \tag{11}$$

where $w(\bar{r}_x)$, $w(\bar{r}_y)$ and $w(\bar{r}_z)$ can be calculated by replacing $\bar{r}$ by $\bar{r}_x$, $\bar{r}_y$ and $\bar{r}_z$ in the expression of $w(\bar{r})$.

2.2. Enforcement of essential boundary conditions

Lacking of Kronecker delta property in EFG shape functions Φ_I poses some difficulty in the imposition of essential boundary conditions. For that different numerical techniques have been proposed to enforce the essential boundary conditions such as Lagrange multiplier method [14,15], modified variational principle approach [17], coupling with finite element method [18], penalty approach [19], full transformation technique [20], etc. In the present work, Lagrange multiplier method has been used due to its accuracy [21,22].

In 3-D, Lagrange multiplier λ is expressed as

$$\lambda(\mathbf{x}) = N_I(a)\lambda_I, \quad \mathbf{x} \in S_i \tag{12a}$$

$$\delta\lambda(\mathbf{x}) = N_I(a)\delta\lambda_I, \quad \mathbf{x} \in S_i \tag{12b}$$

where $N_I(a)$ is a Lagrange interpolant, and a is the area along the essential boundaries.

3. Numerical formulation

In this section, meshless numerical formulation has been presented for a general three-dimensional (3-D) nonlinear, unsteady heat transfer problem (Fig. 1). A general form of energy equation for three-dimensional heat transfer in

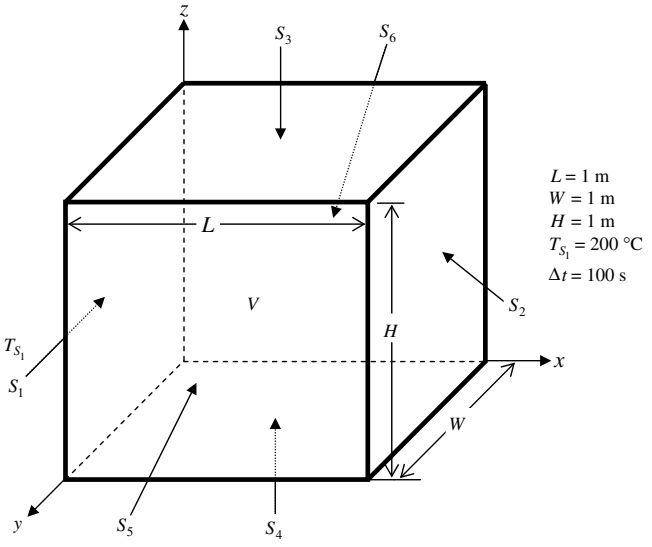

Fig. 1. Three-dimensional model.

isotropic materials with temperature dependent material properties is given as

$$\nabla \cdot \{k(T)\nabla T\} + \dot{Q} = \rho(T)C(T)\dot{T} \tag{13a}$$

with the following initial conditions and boundary conditions

$$T(\mathbf{x},0) = T_i \quad \text{on } V \tag{13b}$$

$$T(\mathbf{x},t) = T_{S_1} \quad \mathbf{x} \in S_1 \tag{13c}$$

$$q(\mathbf{x},t) = h(T - T_\infty) \quad \mathbf{x} \in S_j \tag{13d}$$

where $k(T) = k_0(1+\beta_1 T)$, $\rho(T) = \rho_0(1+\beta_2 T)$, $C(T) = C_0(1-\beta_3 T)$, $j = 2,3,\ldots,6$.

The weak form of Eq. (13a) is obtained as

$$\int_V \nabla\bar{w}\cdot\{k(T)\nabla T\}\mathrm{d}V - \int_V \bar{w}\dot{Q}\mathrm{d}V + \int_V \bar{w}\rho(T)C(T)\dot{T}\,\mathrm{d}V + \sum_{j=2}^{6}\int_{S_j}\bar{w}h(T-T_\infty)\mathrm{d}S = 0 \tag{14}$$

The functional $\Pi(T)$ can be written as

$$\Pi(T) = \frac{1}{2}\int_V \nabla T\cdot\{k(T)\nabla T\}\mathrm{d}V - \int_V T\dot{Q}\mathrm{d}V + \int_V \rho(T)C(T)T\dot{T}\,\mathrm{d}V + \sum_{j=2}^{6}\int_{S_j}\frac{hT^2}{2}\mathrm{d}S - \sum_{j=2}^{6}\int_{S_j} hTT_\infty\mathrm{d}S \tag{15}$$

Enforcing essential boundary conditions using Lagrange multiplier method, the modified functional $\Pi^*(T)$ has been obtained as

$$\Pi^*(T) = \frac{1}{2}\int_V \nabla T.\{k(T)\nabla T\}\mathrm{d}V - \int_V T\dot{Q}\mathrm{d}V + \int_V \rho(T)C(T)T\dot{T}\,\mathrm{d}V + \sum_{j=2}^{6}\int_{S_j}\frac{hT^2}{2}\mathrm{d}S - \sum_{j=2}^{6}\int_{S_j} hTT_\infty\mathrm{d}S + \int_{S_1}\lambda(T-T_{S_1})\mathrm{d}S \tag{16}$$

Taking variation i.e. $\delta\Pi^*(T)$ of Eq. (16), it reduces to

$$\delta\Pi^*(T) = \int_V \nabla T\cdot\{k(T)\delta\nabla T\}\mathrm{d}V - \int_V \dot{Q}\delta T\,\mathrm{d}V + \int_V \rho(T)C(T)\dot{T}\delta T\,\mathrm{d}V + \sum_{j=2}^{6}\int_{S_j} hT\delta T\,\mathrm{d}S - \sum_{j=2}^{6}\int_{S_j} hT_\infty\delta T\,\mathrm{d}S + \int_{S_1}\lambda\delta T\,\mathrm{d}S + \int_{S_1}\delta\lambda(T-T_{S_1})\mathrm{d}S \tag{17}$$

Since δT and $\delta\lambda$ are arbitrary in preceding equation, the following relations are obtained using Eq. (6)

$$[\mathbf{K}(\mathbf{T})]\{\mathbf{T}\} + [\mathbf{M}(\mathbf{T})]\{\dot{\mathbf{T}}\} + [\mathbf{G}]\{\boldsymbol{\lambda}\} = \{\mathbf{f}\} \tag{18a}$$

$$[\mathbf{G}^{\mathrm{T}}]\{\mathbf{T}\} = \{\mathbf{q}\} \tag{18b}$$

where

$$K_{IJ}(T) = \sum_{l=x,y,z}\int_V \Phi_{I,l}k(T)\Phi_{J,l}\mathrm{d}V + \sum_{j=2}^{6}\int_{S_j} h\Phi_I^{\mathrm{T}}\Phi_J\mathrm{d}S \tag{19a}$$

$$M_{IJ}(T) = \int_V \rho(T)C(T)\Phi_I^{\mathrm{T}}\Phi_J\mathrm{d}V \tag{19b}$$

$$f_I = \int_V \dot{Q}\Phi_I\mathrm{d}V + \sum_{j=2}^{6}\int_{S_j} hT_\infty\Phi_I\mathrm{d}S \tag{19c}$$

$$G_{IK} = \int_{S_1}\Phi_I N_K\mathrm{d}S \quad \text{and} \quad q_K = \int_{S_1} T_{S_1}N_K\mathrm{d}S \tag{19d}$$

Applying quasi-linearization, and unconditionally stable implicit backward difference approach [23] for time approximation, Eq. (18) can be written as

$$\begin{bmatrix} [\overline{\mathbf{K}}(\mathbf{T})]^{\bar{n}} + [\mathbf{M}(\mathbf{T})]^{\bar{n}} & \vdots & \mathbf{G} \\ \cdots\cdots & \vdots & \cdots \\ \mathbf{G}^T & \vdots & 0 \end{bmatrix} \begin{Bmatrix} \mathbf{T}^{\bar{n}+1} \\ \boldsymbol{\lambda} \end{Bmatrix} = \begin{Bmatrix} [\mathbf{R}(\mathbf{T})]^{\bar{n}} \\ \mathbf{q} \end{Bmatrix} \tag{20}$$

where $[\mathbf{R}(\mathbf{T})]^{\bar{n}} = [\mathbf{M}(\mathbf{T})]^{\bar{n}}\{\mathbf{T}\}^{\bar{n}} + \Delta t\{\mathbf{f}\}$ and $[\overline{\mathbf{K}}(\mathbf{T})]^{\bar{n}} = \Delta t[\mathbf{K}(\mathbf{T})]^{\bar{n}}$.

4. Numerical results and discussion

In the present work, a general three-dimensional formulation has been provided for a model problem in the previous section. Numerical results have been obtained for nonlinear, unsteady state heat transfer problems with temperature dependent material properties, and it has been assumed that the material parameters namely thermal conductivity, specific heat and density vary linearly with temperature. Quasi-linearization scheme is adopted for the solution of nonlinear equations, and unconditionally-stable backward difference method has been used for the time integration. The EFG results are obtained using linear basis for exponential weight function, whereas FEM results are obtained by ANSYS package. The following data has been used in the present simulations:

Thermal conductivity, $k(T) = k_0(1+\beta_1 T)$, where $k_0 = 400$ W/m °C, $\beta_1 = 0.0001$/°C.
Specific heat, $C(T) = C_0(1+\beta_2 T)$, where $C_0 = 300$ J/kg °C, $\beta_2 = 0.0001$/°C.
Density, $\rho(T) = \rho_0(1-\beta_3 T)$ where, $\rho_0 = 9000$ kg/m^3, $\beta_3 = 0.000001$/°C.
Heat transfer coefficient, $h = 100$ W/m^2 °C.
Surrounding fluid temperature, $T_\infty = 20$ °C.
Initial temperature, $T_i = 0$ °C.

4.1. One-dimensional (1-D) analysis

Three-dimensional formulation has been used for the simulation of one-dimensional, semi-infinite model heat

transfer problem, and it has been assumed that the variation of temperature in semi-infinite solids is one-dimensional but the problem has been modeled in two-dimensional domain as shown in Fig. 2, hence terms containing z have been dropped from 3-D governing equation.

Model data, initial and boundary conditions are also presented in Fig. 2. The EFG results have been obtained using uniform nodal distribution scheme for 42 nodes, whereas FEM results have also been obtained using uniform nodal distribution for the same number of nodes using 20 elements. Fig. 3 shows a comparison of EFG results with those obtained by finite element and analytical methods along the length of model for the various values of time. From the results presented in Fig. 3, it has been

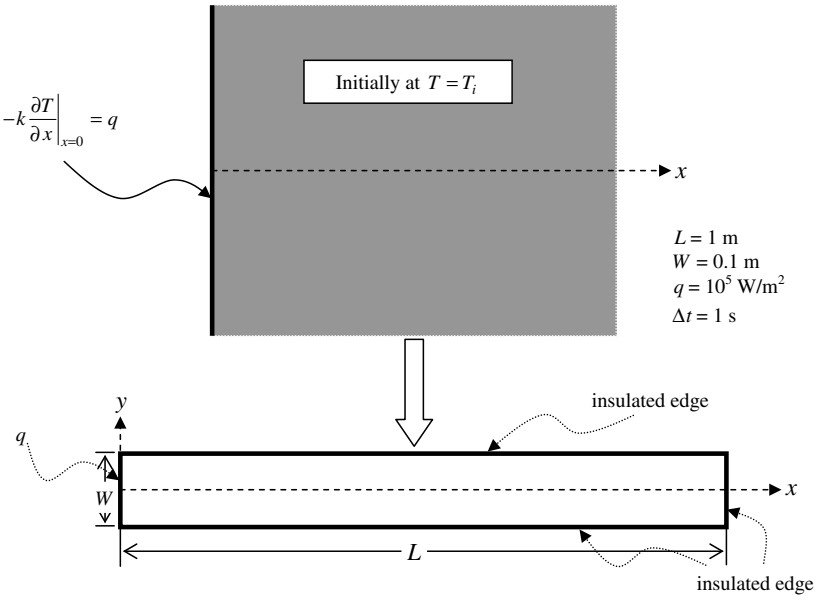

Fig. 2. Semi-infinite model for unsteady-state heat transfer.

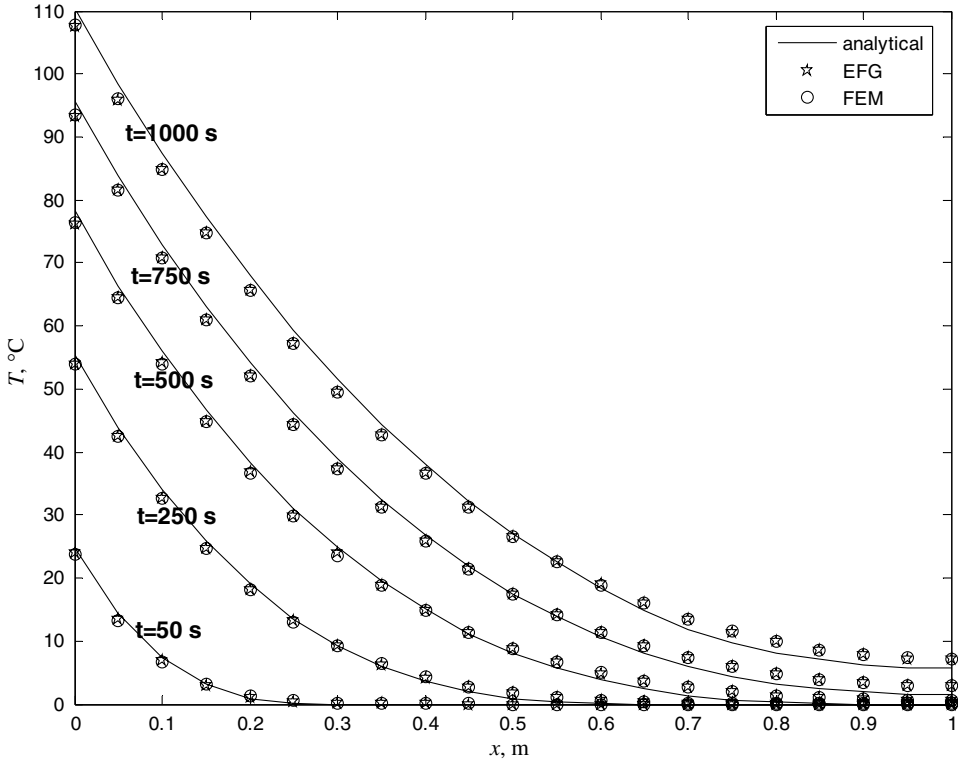

Fig. 3. Comparison of EFG results with analytical and FEM results along length.

observed that the results obtained by EFG method are in good agreement with those obtained by finite element and analytical methods.

4.2. Two-dimensional (2-D) analysis

For 2-D simulation, we consider heat conduction in a unit square as shown in Fig. 4. The left edge of the unit square has been subjected to a constant temperature T_1, and top and right edges are exposed to convection with surrounding fluid temperature T_∞ while bottom edge is kept insulated.

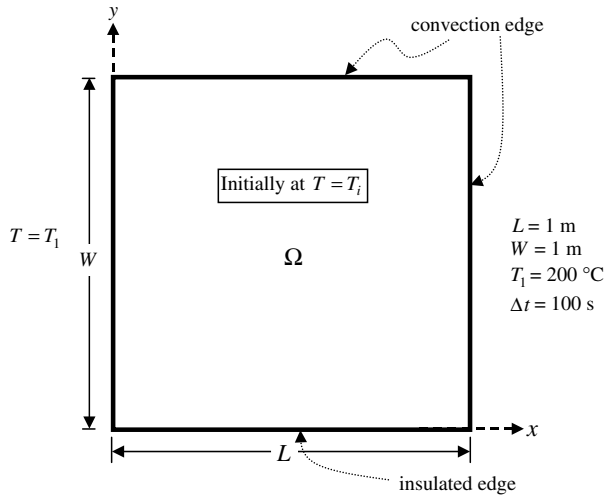

Fig. 4. Two-dimensional model.

3-D formulation has been utilized for 2-D simulation by dropping the terms associated with variable z. FEM results have been obtained by ANSYS package [Version 8.0] using four node quadrilateral element [Plane 55] for a uniform mesh with 121 nodes (100 elements), and EFG results have been obtained using uniform nodal distribution scheme for 121 nodes. A comparison of EFG results with those obtained by finite element method has been presented in Fig. 5 at $(x/L = 0.5, y)$ for $t = 500$ s, 1000 s, 2500 s, 5000 s and 10,000 s. From the results presented in Fig. 5, it can be concluded that the results obtained by EFG method are almost same as those obtained by finite element method.

4.3. Three-dimensional (3-D) analysis

Consider a unit cube (as shown in Fig. 1) for 3-D unsteady-state heat transfer with an initial temperature T_i. The left surface of the cube has been subjected to a constant temperature T_{S_1}, and other surfaces are subjected to convection boundary conditions with surrounding fluid temperature T_∞. The unsteady state EFG results are obtained using uniform nodal distribution scheme for 729 nodes, whereas FEM results are obtained by ANSYS package using 512 elements (3-D brick element, Solid 70) with uniform nodal data distribution scheme for the same number of nodes. A comparison of EFG results with FEM results is presented in Fig. 6 along a line at $(x/L = 0.5, y/W = 0.5, z)$ for $t = 500$ s, 1000 s, 2500 s, 5000 s and

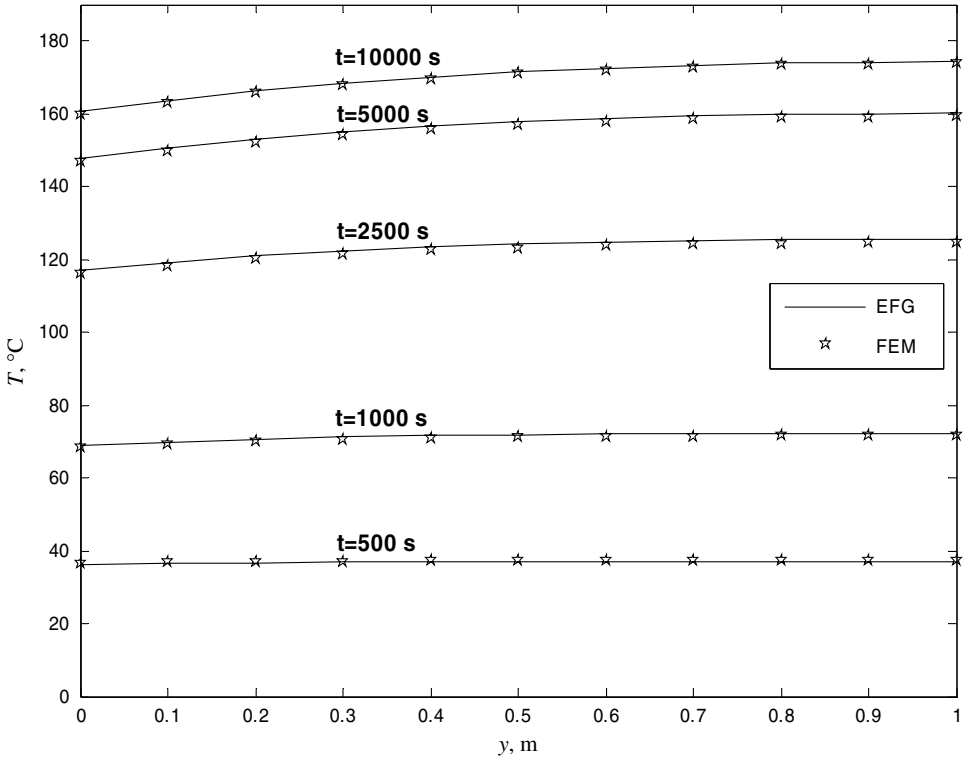

Fig. 5. Comparison of EFG results with FEM results at $(x/L = 0.5, y)$.

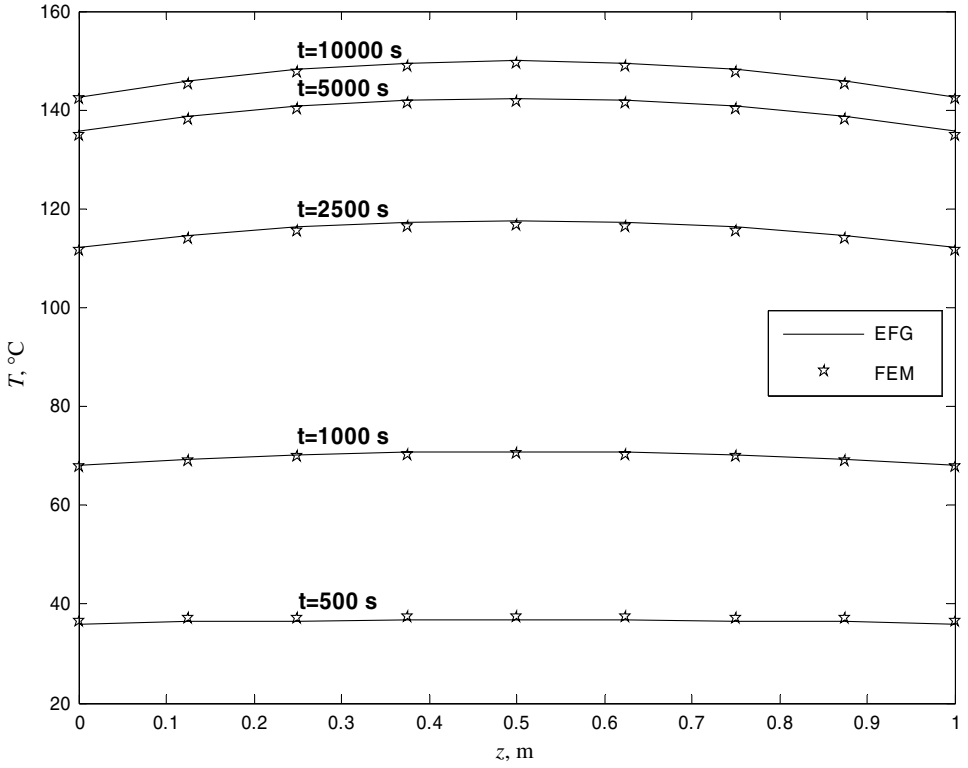

Fig. 6. Comparison of EFG results with FEM results at ($x/L = 0.5$, $y/W = 0.5, z$).

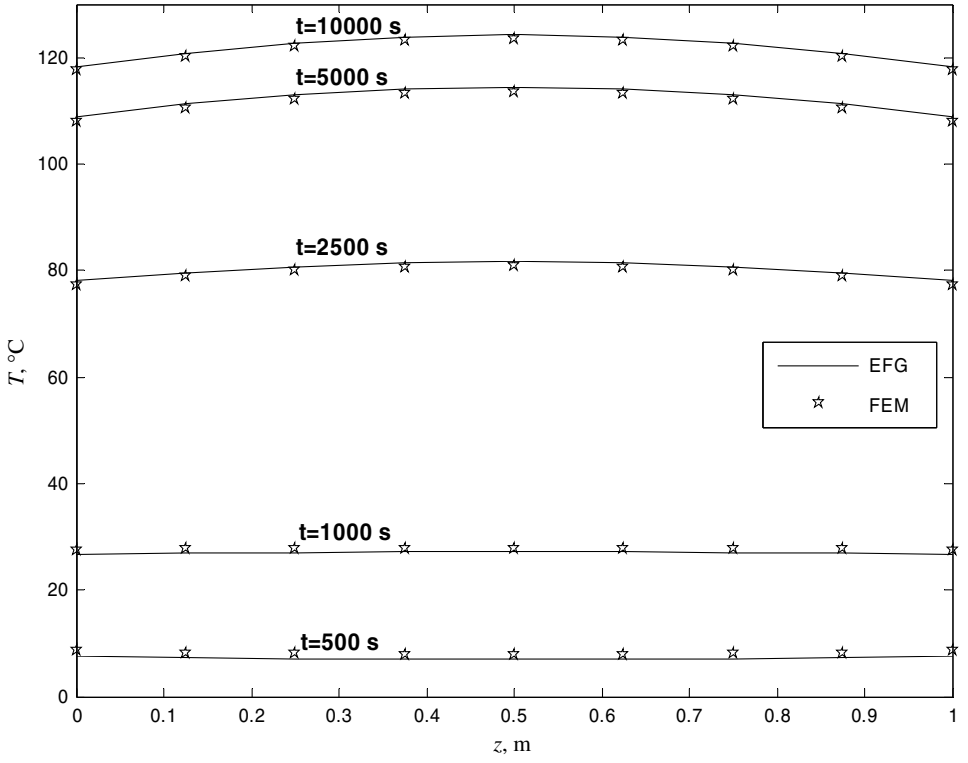

Fig. 7. Comparison of EFG results with FEM results at ($x/L = 1$, $y/W = 0.5, z$).

10,000 s. A similar comparison of EFG results with FEM results is presented in Fig. 7 for the same number of nodes along another line at ($x/L = 1$, $y/W = 0.5, z$). From the results presented in Figs. 6 and 7, it has been observed

that the EFG results are in good agreement with FEM results.

5. Conclusions

In this work, meshless EFG method has been successfully extended to obtain the numerical solution of unsteady state nonlinear heat transfer problems with temperature dependent material properties. It was assumed that the thermal conductivity, specific heat and density vary linearly with temperature. For the linearization of nonlinear equations, quasi-linearization technique was used, whereas for time integration, backward difference method was utilized. In 1-D, the results obtained by EFG method are compared with those obtained by finite element and analytical methods, whereas in 2-D and 3-D, the EFG results are compared with FEM results. From the above analysis, it can be concluded that the results obtained by EFG method are in good agreement with those obtained by FEM results in 1-D, 2-D and 3-D. In future, this work can be extended for the nonlinear heat transfer analysis of the problems having complicated geometries.

References

[1] J. Donea, S. Giuliani, Finite element analysis of steady-state nonlinear heat transfer problems, Nucl. Eng. Des. 30 (1974) 205–213.
[2] K.J. Bathe, M.R. Khoshgoftaar, Finite element formulation and solution of nonlinear heat transfer, Nucl. Eng. Des. 51 (1979) 389–401.
[3] Chung S. Ling, K.S. Surana, *p*-Version least squares finite element formulation for axisymmetric heat conduction with temperature-dependent thermal conductivities, Comput. Struct. 52 (1994) 353–364.
[4] H. Yang, A precise algorithm in the time domain to solve the problem of heat transfer, Numer. Heat Transfer: Part B 35 (1999) 243–249.
[5] S.J. Liao, Numerically solving non-linear problems by the homotopy analysis method, Comput. Mech. 20 (1997) 530–540.
[6] P. Talukdar, S.C. Mishra, Transient conduction and radiation heat transfer with variable thermal conductivity, Numer. Heat Transfer: Part A 41 (2002) 851–867.
[7] Bondarv, Variational method for solving nonlinear problems of unsteady-state heat conduction, Int. J. Heat Mass Transfer 40 (1997) 3487–3495.
[8] S. Liao, General boundary element method for non-linear heat transfer problems governed by hyperbolic heat conduction equation, Comput. Mech. 20 (1997) 397–406.
[9] P. Skerget, A. Alujevic, Boundary element method in nonlinear transient heat transfer of reactor solids with convection and radiation on surfaces, Nucl. Eng. Des. 76 (1983) 47–54.
[10] S.J. Liao, A.T. Chwang, General boundary element method for unsteady non-linear heat transfer problems, Numer. Heat Transfer: Part B 35 (1999) 225–242.
[11] M.R. Siddique, R.E. Khayat, A low-dimensional approach for linear and nonlinear heat conduction in periodic domains, Numer. Heat Transfer: Part A 38 (2000) 719–738.
[12] B. Chen, Y. Gu, Z. Guan, H. Zhang, Nonlinear transient heat conduction analysis with precise time integration method, Numer. Heat Transfer: Part B 40 (2001) 325–341.
[13] G.R. Liu, Y.T. Gu, An Introduction to Meshfree Methods and their Programming, Springer, Netherlands, 2005.
[14] I.V. Singh, K. Sandeep, R. Prakash, The element free Galerkin method in three-dimensional steady state heat conduction, Int. J. Comput. Eng. Sci. 3 (2002) 291–303.
[15] I.V. Singh, Meshless EFG method in 3-D heat transfer problems: a numerical comparison, cost and error analysis, Numer. Heat Transfer: Part A 46 (2004) 199–220.
[16] M.N. Özisik, Heat Conduction, second ed., John Wiley and Sons, Singapore, 1993.
[17] M. Fleming, Y.A. Chu, B. Moran, T. Belytschko, Enriched element free Galerkin methods for crack tip fields, Int. J. Numer. Methods Eng. 40 (1997) 1483–1504.
[18] Y. Krongauz, T. Belytschko, Enforcement of essential boundary conditions in meshless approximations using finite elements, Comput. Methods Appl. Mech. Eng. 131 (1996) 133–145.
[19] G.R. Liu, X.L. Chen, J.N. Reddy, Buckling of symmetrically laminated composite plates using the element-free Galerkin method, Int. J. Struct. Stab. Dyn. 2 (2002) 281–294.
[20] B.N. Rao, S. Rahman, An efficient meshless method for fracture analysis of cracks, Comput. Mech. 26 (2000) 398–408.
[21] T. Belytschko, Y.Y. Lu, L. Gu, Element-free Galerkin methods, Int. J. Numer. Methods Eng. 37 (1994) 229–256.
[22] T. Belytschko, Y.Y. Lu, L. Gu, Crack propagation by element free Galerkin methods, Eng. Fract. Mech. 51 (1995) 295–315.
[23] J.N. Reddy, D.K. Gartling, The Finite Element Method in Heat Transfer and Fluid Dynamics, second ed., CRC Press, USA, 2001.